Identification of Axl as a downstream effector of TGF-β1 during Langerhans cell differentiation and epidermal homeostasis

Thomas Bauer,[1,2] Anna Zagórska,[3] Jennifer Jurkin,[1] Nighat Yasmin,[1] René Köffel,[1,2] Susanne Richter,[1] Bernhard Gesslbauer,[1] Greg Lemke,[3,4] and Herbert Strobl[1,2]

[1]Institute of Immunology, Center of Pathophysiology, Infectiology, and Immunology, Medical University of Vienna, 1090 Vienna, Austria
[2]Institute of Pathophysiology and Immunology, Center of Molecular Medicine, Medical University Graz, 8010 Graz, Austria
[3]Molecular Neurobiology Laboratory and [4]Immunobiology and Microbial Pathogenesis Laboratory, Salk Institute for Biological Studies, La Jolla, CA 92037

Transforming growth factor–β1 (TGF–β1) is a fundamental regulator of immune cell development and function. In this study, we investigated the effects of TGF–β1 on the differentiation of human Langerhans cells (LCs) and identified Axl as a key TGF–β1 effector. Axl belongs to the TAM (Tyro3, Axl, and Mer) receptor tyrosine kinase family, whose members function as inhibitors of innate inflammatory responses in dendritic cells and are essential to the prevention of lupus–like autoimmunity. We found that Axl expression is induced by TGF–β1 during LC differentiation and that LC precursors acquire Axl early during differentiation. We also describe prominent steady–state expression as well as inflammation–induced activation of Axl in human epidermal keratinocytes and LCs. TGF–β1–induced Axl enhances apoptotic cell (AC) uptake and blocks proinflammatory cytokine production. The antiinflammatory role of Axl in the skin is reflected in a marked impairment of the LC network preceding spontaneous skin inflammation in mutant mice that lack all three TAM receptors. Our findings highlight the importance of constitutive Axl expression to tolerogenic barrier immunity in the epidermis and define a mechanism by which TGF–β1 enables silent homeostatic clearing of ACs to maintain long–term self–tolerance.

The Journal of Experimental Medicine

CORRESPONDENCE
Herbert Strobl:
herbert.strobl@meduniwien.ac.at

Abbreviations used: Ab, antibody; AC, apoptotic cell; BMDC, BM-derived DC; BMDM, BM-derived macrophage; CHS, contact hypersensitivity; DNFB, 2,4 dinitro-1-fluorobenzene; FLT3L, fms-related tyrosine kinase 3 ligand; LC, Langerhans cell; moDC, monocyte–derived DC; moLC, monocyte–derived LC; mRNA, messenger RNA; SCF, stem cell factor; TLR, Toll-like receptor.

TGF-β1 is a potent immunosuppressive cytokine that controls steady-state immune homeostasis, the resolution of inflammatory responses, and the maintenance of self-tolerance (Li et al., 2006). This is reflected in the phenotypes displayed by TGF-β1–null mice, which develop lethal multifocal inflammation and autoantibody (auto-Ab) production (Shull et al., 1992; Dang et al., 1995). TGF-β1 is especially important in the establishment and maintenance of skin immunity (Li et al., 2006; Ueno et al., 2007). A tight regulation of skin immune responses is necessary for both protection against pathogens and prevention of overreactions to commensals or environmental stress at the body surface.

The outermost layer of the skin, the epidermis, harbors a tight network of DCs, known as Langerhans cells (LCs; Ueno et al., 2007). TGF-β1 controls LC homeostasis in the steady state by preventing their spontaneous maturation

and emigration from the epidermis (Kel et al., 2010). Apart from its role in the maintenance of an immature phenotype, TGF-β1 in the skin microenvironment is crucial for LC development (Li et al., 2006). TGF-β1 induces LC differentiation via paracrine and autocrine production from suprabasal keratinocytes and LCs, respectively (Kaplan et al., 2007). TGF-β1–null mice lack LCs (Borkowski et al., 1996), and LC differentiation can be induced by TGF-β1 in vitro from both human hematopoietic stem cells (Strobl et al., 1996) and monocytes (Geissmann et al., 1998).

Axl belongs to the TAM (Tyro3, Axl, and Mer) receptor tyrosine kinase family, whose members are essential to the homeostatic clearance of
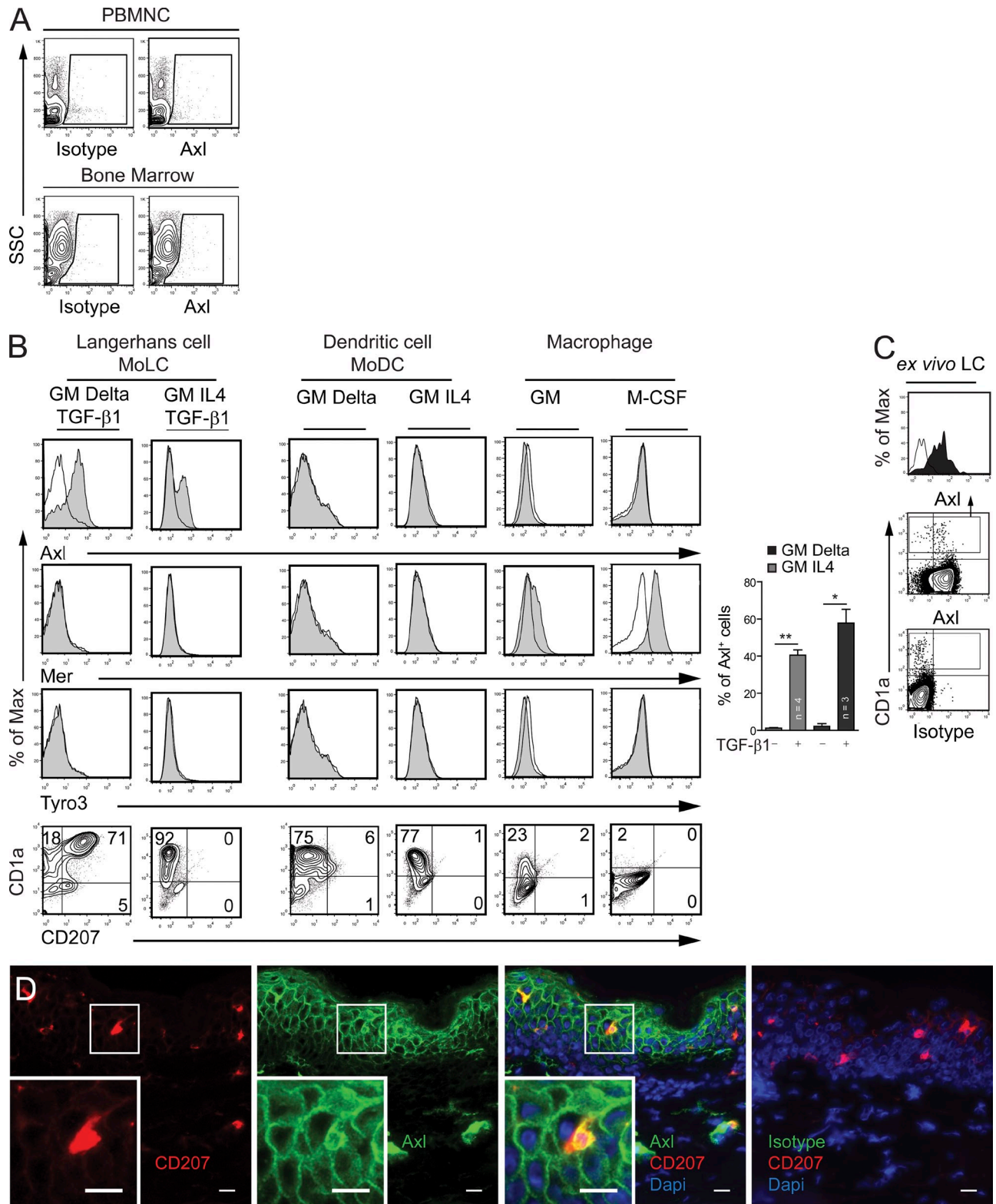
Figure 1. Axl is specifically expressed on human LCs and epidermal keratinocytes. (A) Human PBMCs and BM cells were stained for Axl or isotype control. Data are representative of three different donors and experiments. (B) Human peripheral blood monocytes were differentiated for 5 d with the indicated cytokines and ligands (GM, GM-CSF; Delta, Delta-like-1) and were then analyzed for the expression of the TAM receptors and surface markers. Data are representative of at least three donor experiments. Open histograms represent isotype control, and filled histograms represent specific staining. Bars represent mean (±SEM) percentage of Axl-positive cells. Replicate number (n) is indicated in the bars. *, P < 0.05; **, P < 0.01. (C) FACS analyses of

apoptotic cells (ACs; Lemke and Burstyn-Cohen, 2010). Mice lacking all three receptors (Tyro3, Axl, and Mer) have several degenerative phenotypes linked to inefficient removal of ACs and membranes (e.g., in the retina and the male reproductive tract) and develop a severe autoimmune phenotype similar to systemic lupus erythematosus, including the production of broad spectrum auto-Abs (Lu et al., 1999; Lu and Lemke, 2001).

In addition to their role in phagocytosis of ACs, TAM receptors, especially Axl, have been implicated in inhibiting proinflammatory Toll-like receptor (TLR) responses (Sharif et al., 2006; Rothlin et al., 2007). During inflammation, Axl is strongly induced via type I IFNs triggered by TLR stimulation of DCs and macrophages and when activated provides a negative feedback signal to shut down the immune response (Sharif et al., 2006; Rothlin et al., 2007). Even though the TAM receptors are responsible for maintaining long-term self-tolerance, the molecular mechanisms underlying their normal homeostatic expression remain elusive (Lu and Lemke, 2001).

As the mechanisms governing LC differentiation and maturation in response to TGF-β1 signaling remain for the most part unclear, we made use of a defined serum-free human in vitro LC differentiation model to identify key effector molecules. We found Axl to be strongly induced concomitant with TGF-β1–dependent LC differentiation from human hematopoietic progenitors. Because specific signals that regulate TAM receptor expression are not known and because both the TAM system and TGF-β1 have been independently shown to represent critical negative regulators of immune responses, we considered the here identified TGF-β1–dependent Axl induction of considerable relevance. Our data demonstrate a mechanism by which TGF-β1 regulates and utilizes the TAM receptors during DC/macrophage differentiation and implicate the TAM system in epidermal homeostasis.

RESULTS
Axl is strongly expressed by LCs
We performed gene array profiling of human monocyte progenitor cells undergoing LC differentiation. The TAM receptor Axl was among the strongest induced genes in LC committed progenitors (not depicted). To investigate whether Axl expression is specific for LCs, we performed systematic expression analyses among hematopoietic cells. Axl is not expressed by human granulocytes, monocytes, or lymphocytes isolated from either peripheral blood or BM (Fig. 1 A). Conversely, in vitro–generated monocyte-derived CD207+ LCs (in response to GM-CSF, Delta-1, and TGF-β1) strongly expressed Axl (Fig. 1 B, histograms and bar diagram). Similarly, Axl was detectable on LCs generated in the presence of GM-CSF, IL-4, and TGF-β1

(Fig. 1 B, histograms and bar diagram). These cells were previously shown to exhibit LC features such as E-cadherin and high CD1a expression (Geissmann et al., 1998). Conversely, neither monocyte-derived DCs (moDCs; GM-CSF, IL-4 or GM-CSF, Delta-1; generated in the absence of TGF-β1) nor monocyte-derived macrophages (M-CSF or GM-CSF) expressed Axl at detectable levels (Fig. 1 B, histograms and bar diagram). FACS and immunohistology confirmed that LCs in vivo express Axl (Fig. 1, C and D). Additionally, keratinocytes also exhibited strong membrane staining for Axl, with Axl expression gradually increasing from basal to suprabasal epidermal layers (Fig. 1 D). In contrast to Axl, the other two TAM family members Tyro3 and Mer were not induced during LC differentiation. Moreover, moDCs and cells from peripheral blood and BM including monocytes lacked all three receptors (Fig. 1 B and not depicted). However, Mer but not Tyro3 was found to be induced concomitant with macrophage differentiation in the presence of either M-CSF or GM-CSF, in keeping with the previous demonstration that Mer is crucial for AC uptake by macrophages (Fig. 1 B, histograms; Scott et al., 2001). Therefore, among the hematopoietic cells analyzed, Axl was specifically expressed by LCs and was the only TAM receptor constitutively expressed among the human moDC subsets studied.

Keratinocytes express TAM receptor ligands Gas6 and Protein S
Given the strong and specific expression of Axl by LCs, we next investigated whether Axl ligands are expressed in the epidermis. Gas6 is the predominant ligand for Axl (Nagata et al., 1996). Immunohistology revealed a high expression intensity of Gas6 by keratinocytes. Interestingly, Gas6 is expressed by the suprabasal keratinocytes but not by the basal keratinocyte layer (Fig. 2 A), thus showing a similar expression pattern as observed for Axl (Fig. 1 D). The other TAM receptor ligand, Protein S (Stitt et al., 1995), which is thought to function primarily as a ligand for Mer and Tyro3, was also detectable in keratinocytes; however, it showed an inverse expression pattern, with basal layers exhibiting higher Protein S expression (Fig. 2 B). Therefore, TAM ligands are abundantly expressed in the epidermis.

Axl is rapidly induced during early LC commitment
We used CD34+ hematopoietic progenitor/stem cells from human umbilical cord blood to study Axl induction during DC subset differentiation. GM-CSF/IL4-dependent DCs generated in vitro from CD34+ cells via a two-step culture system (Ratzinger et al., 2004) lacked TAM receptor expression in keeping with the observed absence of these receptors

human epidermal single cell suspensions stained for Axl or isotype control. LCs were identified as CD1a+ cells. The filled histogram represents specific staining, and the open histogram represents isotype control. One representative experiment out of three different donors and experiments is shown. (D) Immunohistochemistry of human adult skin cryosections for Axl and CD207. Nuclei were visualized with DAPI. Colors are as indicated. Data are representative of at least three different donors and experiments. The insets show an enlarged view of the framed areas. Section thickness was 5 µm. Bars, 10 µm.
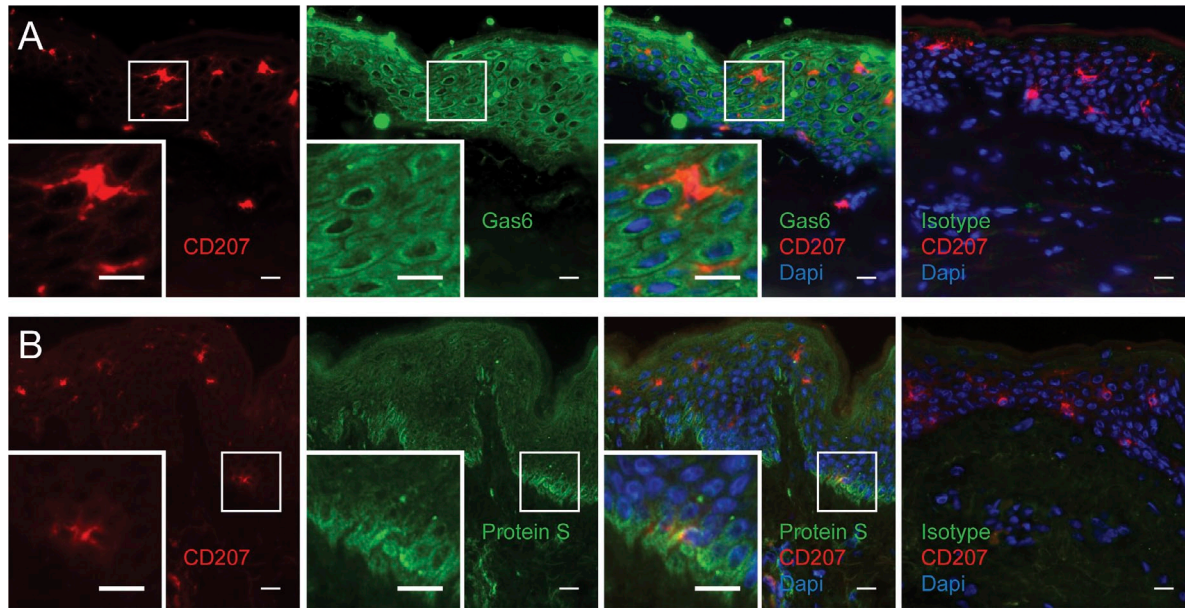
Figure 2. TAM receptor ligands Gas6 and Protein S are expressed in the human epidermis. (A and B) Immunohistochemistry of human adult skin cryosections for Gas6 (A) and Protein S (B). Pictures are representative of at least three different donors and experiments. LCs were visualized with Abs against CD207, and nuclei with DAPI. Colors are as indicated. The insets show an enlarged view of the framed areas. Section thickness was 5 µm. Bars, 10 µm.

by moDCs (Figs. 3 A and 1 B). In contrast, in vitro–generated CD34+ cell–derived LCs were Axl+ (Fig. 3, B and C). Specifically, Axl expression was only seen under TGF-β1–dependent LC instructive lineage differentiation conditions (Fig. 3 B, bar diagram). Time kinetic analyses revealed that LC precursors first acquire Axl (day 4), followed by the induction and subsequent up-regulation of CD1a (days 4–7; Fig. 3 C, right). Moreover, most Axl+ cells coexpressed CD324 (E-cadherin) at days 4 and 7 during LC differentiation (Fig. 3 C, + TGF-β1). Unlike as observed for Axl, the other TAM receptors Mer and Tyro3 are not induced concomitant with TGF-β1–dependent LC differentiation (Fig. 3 C, histograms).

Enrichment of LC differentiation potential in Axl–positive precursor cells

To verify that Axl is expressed by LC precursors, we performed cell sorting experiments. A robust Axl+ cell population could be distinguished from Axl− cells already at day 3 in LC generation cultures initiated from CD34+ cells, allowing the isolation of Axl+ and Axl− cell fractions (Fig. 4 A, histogram). After 4 d of further subcultivation under LC differentiation conditions (i.e., in the presence of TGF-β1, day 7 generated cells), cell volume and granularity were increased in cells derived from the sorted Axl+ cells as compared with cells from the Axl− fraction (Fig. 4 A, plot). Cultures initiated with Axl+ cells showed typical LC clusters, which are known to be dependent on E-cadherin adhesion (Fig. 4 A, bright field picture, arrowheads; Tang et al., 1993; Riedl et al., 2000). Conversely cultures initiated by the Axl− fraction remained as single cells (Fig. 4 A, right bright field picture). As expected from their LC-like

morphology, FACS analysis revealed the typical LC surface marker expression profile (CD207+CD1a+CD324+) by cells derived from the Axl+ fraction (Fig. 4 B). Further subcultivation of day 3 Axl+ cells without the addition of TGF-β1 revealed that high expression levels of the LC marker CD207 are dependent on the continuous presence of TGF-β1 from days 3 to 7 (Fig. 4 B, top left). Similarly, Axl surface levels diminished during culture in the absence of TGF-β1, indicating that the continued presence of TGF-β1 from days 3 to 7 is required to maintain Axl surface expression (Fig. 4 C). LC differentiation from sorted day 3 Axl+ precursors occurred in the absence of cell proliferation, whereas Axl− precursors continued to proliferate under identical cytokine conditions (Fig. 4 B, bottom right). In the absence of TGF-β1, day 3 sorted Axl+ cells still proliferated to a similar extent as observed for Axl− precursors (Fig. 4 B, bottom right). In aggregate, these observations indicate that Axl is acquired early during LC differentiation from CD34+ hematopoietic progenitor cells in response to TGF-β1 and that the continued presence of TGF-β1 is required to maintain Axl expression along with LC markers.

Axl messenger RNA (mRNA) expression is mediated by TGF-β1 without the need for de novo protein synthesis during LC lineage commitment

Because we observed that Axl expression is induced during TGF-β1–dependent LC differentiation and that continuous TGF-β1 is required for the maintenance of Axl expression (Fig. 3, B and C; and Fig. 4 C), we investigated whether TGF-β1 signaling has a direct effect on the Axl
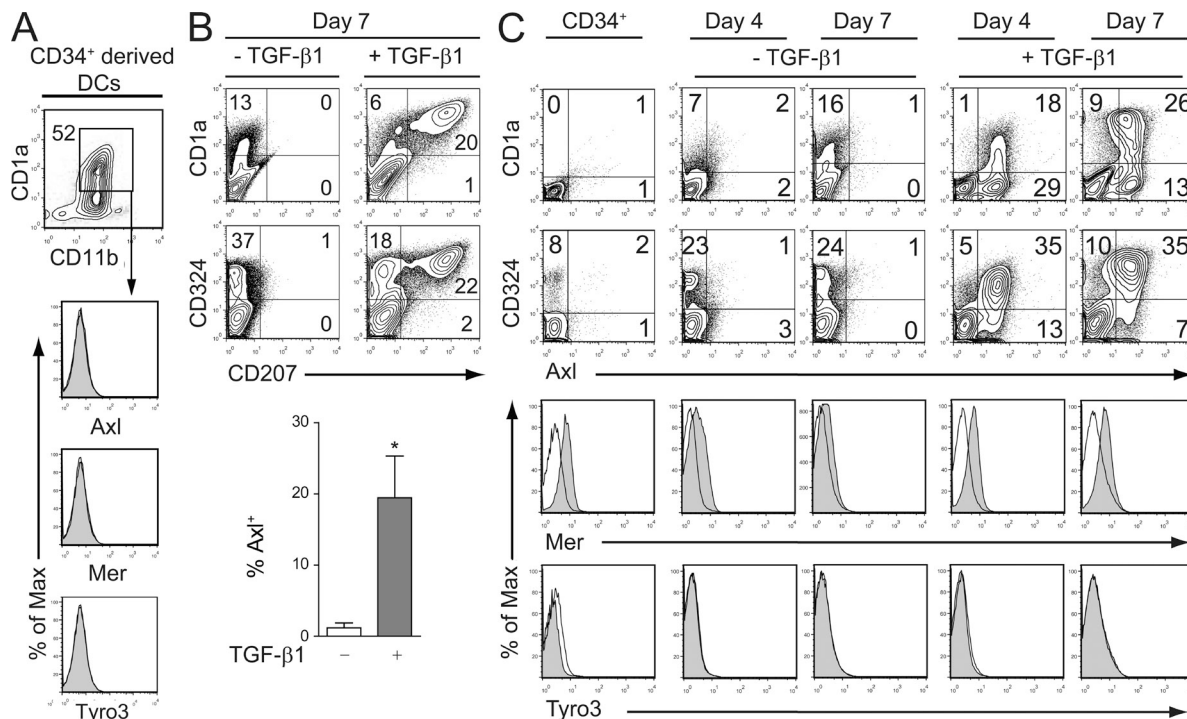
Figure 3. Axl is rapidly induced during early LC commitment. (A) CD34+ cells were cultured using a two-step DC-promoting culture system containing GM-CSF and IL-4 in the final step. Gated CD1a+CD11b+ cells were analyzed for the expression of the TAM receptors. Data are representative of three independent experiments. (B) CD34+ cells were cultured for 7 d in serum-free medium containing LC-promoting cytokine cocktail (GM-CSF, SCF, FLT3L, TNF, and TGF-β1). Parallel cultures were initiated without TGF-β1. Data are representative of at least three independent experiments. Bars represent the mean of percentages (±SEM) of cells Axl positive observed at days 3–4 from the total cell population (n = 6 donors). *, P < 0.05. (C) TAM surface expression on fresh CD34+ cells as well as by cells undergoing TGF-β1–dependent LC differentiation (days 4 and 7). Parallel cultures were initiated without TGF-β1. One representative out of three independent experiments is shown. Open histograms represent isotype control, and filled histograms represent specific staining as indicated.

mRNA levels during LC commitment. Therefore we induced CD34+ cells to undergo LC differentiation in response to TGF-β1 stimulation as described previously (Strobl et al., 1997). An ∼40-fold mRNA increase could be observed already after 6 h of TGF-β1 stimulation in progenitor cells under LC instructive stimulation conditions; this further increased up to 250-fold after 24 h relative to parallel cultures without TGF-β1 (Fig. 4 D). The addition of the protein synthesis inhibitor cycloheximide together with TGF-β1 failed to abolish Axl mRNA levels at 6 h, indicating that LC-specific Axl expression downstream of TGF-β1 signaling does not require new protein synthesis (Fig. 4 D, dark bar).

TGF-β1–induced Axl inhibits TLR-mediated LC activation

Because keratinocytes express Gas6 (Fig. 2 A), LCs are constantly exposed to this ligand. We therefore studied whether Gas6 influences LC activation/maturation via Axl similarly as previously reported for mouse BM-derived DCs (BMDCs; Rothlin et al., 2007). Indeed, the addition of Gas6 inhibited TLR2-mediated up-regulation of the activation markers CD86 and CD83 by LCs (Fig. 5 A, histograms). The addition of an anti-Axl blocking Ab before Gas6 stimulation

abrogated the inhibitory effect of Gas6 on phenotypic LC maturation (Fig. 5 A, histograms). In line with this, Gas6 inhibited TLR2-mediated proinflammatory cytokine release (TNF and IL12p40) by LCs, and this effect was counteracted by anti-Axl pretreatment (Fig. 5 A, bar diagrams). Therefore, TGF-β1–induced Axl inhibits TLR2-mediated LC maturation. Because it has previously been shown that the TAM ligands Protein S and Gas6 are present in cell culture media, because of Protein S–rich serum and autocrine secretion (Anderson et al., 2003), we next studied functional consequences of the continuous presence of Axl-blocking Abs during LC cultures initiated by CD14+ monocytes (Anderson et al., 2003). Unlike CD34+ cell–derived LC generation cultures (Strobl et al., 1997), these monocyte-derived LC (moLC) cultures crucially depend on serum supplementation (not depicted). Anti-Axl Ab promoted TLR2-induced up-regulation of CD86 and CD83 (Fig. 5 B); moreover, anti-Axl promoted TLR-dependent induction of proinflammatory cytokines TNF, IL-6, and IL-12p40 (Fig. 5 C). Therefore, inhibition of endogenous Axl signaling during LC differentiation results in the generation of cells exhibiting an enhanced capacity to undergo TLR-dependent maturation.
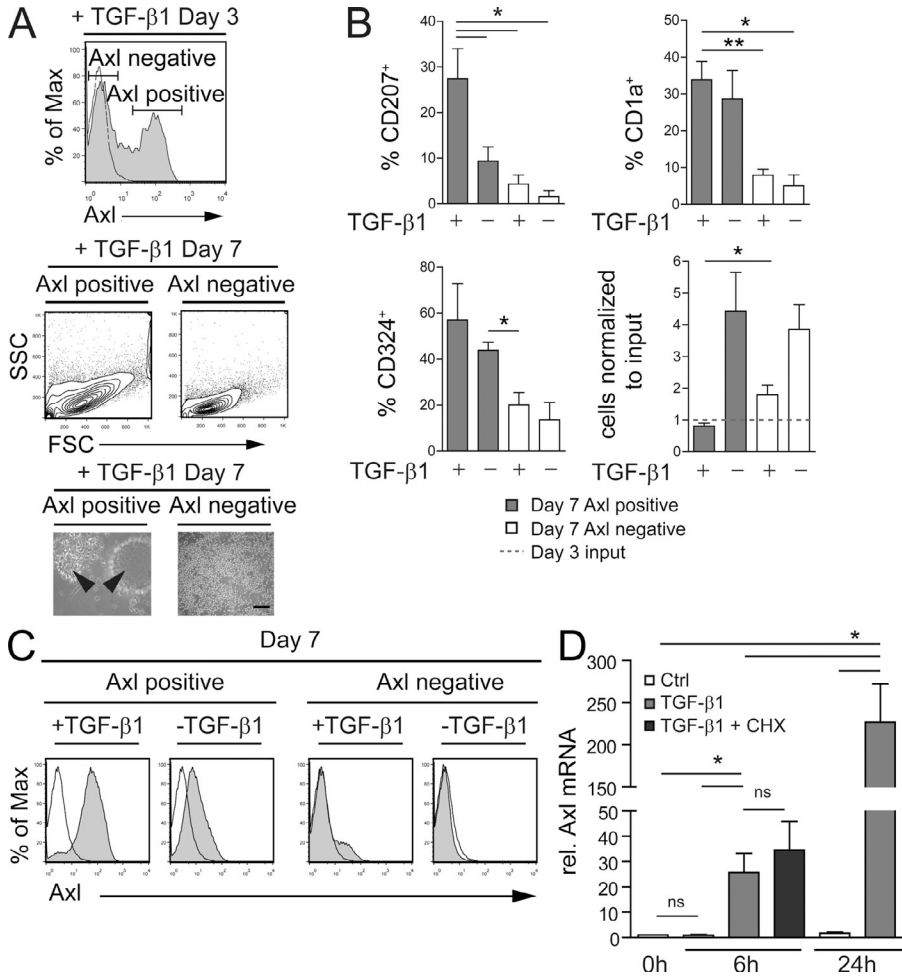
Figure 4. Axl is expressed early during LC differentiation downstream of TGF-β1 signaling. (A) CD34^{+} cells were cultured for 3 d in serum-free medium containing an LC-promoting cytokine cocktail (GM-CSF, SCF, FLT3L, TNF, and TGF-β1). FACS sort windows of Axl positive/negative ([+/−]) cells on day 3 are indicated. The open histogram represents isotype control. Lower plots and bright field microscope pictures represent size properties (SSC and FSC) and cluster formation of sorted Axl^{+/−} cells after 4 d of reculture. Representative data from six different experiments and donors are shown. Arrowheads (bottom left bright field picture) indicate representative cell clusters. Bar, 50 µm. (B) Surface marker expression and normalized cell counts of 4-d-recultured Axl^{+/−} cells ± TGF-β1. Bars represent the mean (±SEM) of three (bottom) to six (top) different reculture experiments with different donors. (C) Representative FACS histograms of 4-d-recultured Axl^{+/−} cells ± TGF-β1 stained for Axl surface expression. Data are representative of three independent experiments. Open histograms represent isotype control, and filled histograms represent specific staining. (D) Axl mRNA expression after 6 and 24 h of culture ± TGF-β1, relative to 0 h measured by quantitative real-time RT-PCR. Values were normalized to HPRT. Cycloheximide (CHX) was added 1 h before TGF-β1 in parallel cultures for 6 h. Bars represent mean (±SEM). Data represent four different donor experiments. *, $P < 0.05$; **, $P < 0.01$.

## TGF-β1–induced Axl confers enhanced capability for uptake of ACs

The TAM receptor system (especially Mer) is known to be involved in the phagocytosis of ACs during tissue homeostasis as well as during the resolution of inflammation (Lemke and Burstyn-Cohen, 2010). We first analyzed a possible involvement of Axl in the phagocytosis of ACs by human LCs derived from CD34^{+} cells using a FACS-based assay (Fig. 6 A). Indeed, anti-Axl Abs diminished the uptake of PKH26-labeled ACs by LCs observed in three independent experiments (Fig. 6, A and B). Because macrophages produce elevated levels of TGF-β1 upon AC uptake (Huynh et al., 2002) and Axl is induced by TGF-β1, we assessed the possibility that Axl may mediate enhanced phagocytic capacity of TGF-β1–stimulated phagocytes. To investigate the contribution of Axl to AC uptake in response to TGF-β1 stimulation, we used M-CSF–dependent mouse BM-derived macrophages (BMDMs) genetically deficient for the TAM receptors. The addition of TGF-β1 during WT but not TAM^{−/−} macrophage cultures resulted in the strong induction of Axl expression (from almost undetectable levels) at both the protein and mRNA levels (Fig. 6, C and D). In contrast to Axl, Mer expression levels of WT macrophages

generated with or without TGF-β1 remained equivalent (Fig. 6, C and D). Moreover, Tyro3 was not detectable in both conditions (not depicted). TGF-β1–treated macrophages showed substantially enhanced phagocytic capacity as compared with control macrophages (Fig. 6, E and F). This effect was abrogated when analyzing cells generated in parallel from Axl single- or TAM triple–deficient mice (Fig. 6, E and F). Therefore, Axl is required for the observed TGF-β1–mediated enhancement of phagocytosis by macrophages.

TGF-β1 signaling regulates TAM expression pattern by mouse BMDCs

We next analyzed whether the basal Axl expression in mouse DCs is similarly regulated by TGF-β1. DCs were generated from mouse BM in the presence of GM-CSF with or without TGF-β1. In line with previous observations, BMDCs expressed Axl (Fig. 7 A; Rothlin et al., 2007; Seitz et al., 2007). Addition of TGF-β1 to these cultures resulted in enhanced Axl expression, whereas inhibiting TGF-β receptor type I and II signaling using inhibitor LY2109761 completely abrogated basal and induced Axl expression, therefore indicating that Axl expression by mouse BMDCs is mediated via endogenous
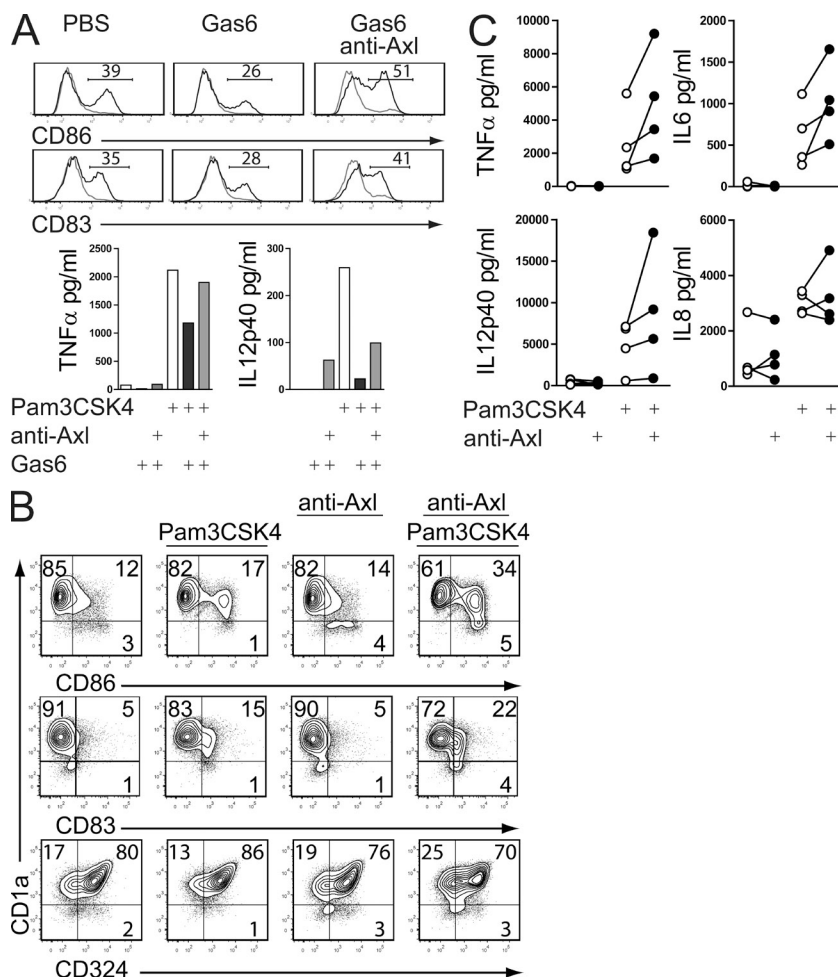
Figure 5. TGF–β1–induced Axl impairs TLR-mediated LC activation. (A) MoLCs were incubated with an anti-Axl blocking Ab or isotope control for 1 h, then stimulated with 400 ng/ml Gas6 or PBS for 3 h, and activated with PAM₃CSK₄ for another 20 h. Thin lines represent control, and thick lines represent activated cells. FACS analysis for the indicated surface markers is shown in the top plots. Bottom bars represent cytokine concentrations measured in the supernatants by LUMINEX. A representative experiment from two different donors and experiments is shown. (B and C) MoLCs were differentiated in the presence GM-CSF, IL-4, TGF–β1, and 5 µg/ml anti-Axl blocking Ab or isotype control for 5 d and subsequently activated with PAM₃CSK₄ for 20 h. A representative experiment out of four different donor experiments is shown. (C) Cytokine levels in the supernatants were measured by LUMINEX. Dots represent the four different donor experiments performed. Open dots indicate isotype control; closed dots indicate blocking anti-Axl Ab.

three TAM receptors independently, with Axl strongly and Mer modestly up-regulated, whereas Tyro3 is down-regulated.

## Axl induction downstream of TLR signaling occurs independently of TGF–β1

It is known that Axl is induced by TLR activation in DCs and macrophages, thus providing negative feedback control of proinflammatory cytokine production (Sharif et al., 2006; Rothlin et al., 2007). Because we here described that the Axl expression is mediated by TGF–β1 during LC, DC, and macrophage differentiation (Figs. 1, 4, 6, and 7), we analyzed whether TLR–induced Axl is similarly dependent on TGF–β1. As expected (Rothlin et al., 2007), LPS stimulation of mouse macrophages resulted in strong Axl induction (Fig. 7 D). The addition of TGF–β1 inhibitor LY2109761 failed to interfere with Axl induction by LPS (Fig. 7 D). Therefore, TLR–mediated Axl up-regulation is independent of TGF–β1 signaling, indicating that these two pathways regulating Axl (i.e., TGF–β1 vs. TLR mediated) in DCs and macrophages are at least in part distinct.

Loss of LC network integrity in TAM–deficient mice precedes skin inflammation

LCs in vivo depend on TGF–β1 signaling, and a conditional deletion of TGF–β receptor I in LCs results in the hyperactivation and spontaneous gradual loss of LCs within 10 d after birth (Kel et al., 2010). Because we observed that among the TAM receptors Axl is selectively expressed at high levels by LCs (Fig. 1, B and C) and that it is induced/maintained in LCs downstream of TGF–β1 signaling (Fig. 3, B and C; and Fig. 4, C and D), we asked whether the loss of Axl results in diminished LC maintenance. Analysis of mouse skin sections revealed a similar Axl expression pattern

TGF–β1 (Fig. 7 A). Interestingly, blocking endogenous TGF–β1 signaling resulted in the strong induction of Tyro3, reciprocally to the loss of Axl (Fig. 7 A). Mer levels were also diminished upon blocking TGF–β1 signaling (Fig. 7 A). Similar results were obtained by blocking TGF–β receptor I signaling alone using SB431542 (Fig. 7 B). Therefore, endogenous TGF–β1 in BMDC cultures induces Axl expression at the expense of Tyro3. We subsequently studied whether the absence of one of the three TAM family members in DCs results in compensatory up-regulation of the other two receptors. Indeed, single absence of Axl or Mer or Tyro3 during BMDC cultures resulted in a modest counter–up-regulation of the other two receptors (Fig. 7 C). This opens the possibility that the aforementioned induction of Tyro3 in response to abrogated TGF–β1 signaling is partially mediated by the absence of Axl (Fig. 7, A–C). However, the alterations in TAM expression by TGF–β1 signaling cannot be solely attributed to changes in Axl as the observed strong Tyro3 up-regulation in TGF–β1 signaling–blocked DC cultures exceeds the observed weak Tyro3 induction in Axl-deficient DCs (Fig. 7, A–C). Additionally, Mer is enhanced in Axl-deficient DCs but is diminished in TGF–β1 signaling–blocked DCs (Fig. 7, A–C). These observations suggest that TGF–β1 can regulate all
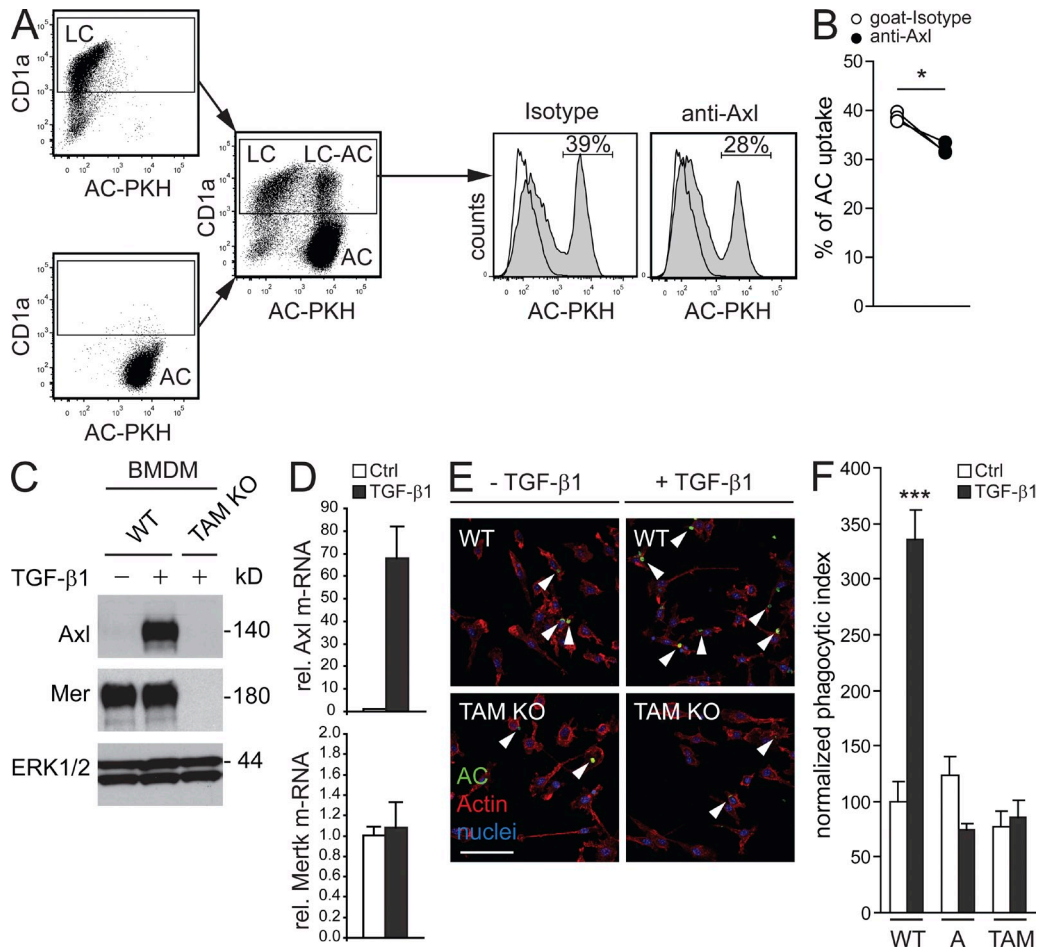
Figure 6. TGF-β1–induced Axl confers enhanced capability for uptake of ACs. (A) Cluster-purified CD34^{+} derived LCs were incubated for 90 min with PKH26-labeled ACs at 37°C before FACS analysis. LCs were incubated with 5 µg/ml anti-Axl blocking Ab or isotype control 30 min before AC exposure. CD1a^{+} cells were analyzed for PKH26. PKH26-positive LCs are depicted as a percentage (FACS histograms). Data are representative of three independent experiments performed with different donors. (B) Graph represents data analyzed as described in A from three different experiments with different donors. (C) BM from WT and TAM KO mice was cultured in the presence of M-CSF ± 0.25 ng/ml TGF-β1 for 7 d and analyzed for Axl and Mer expression by Western blot. One representative out of six independent experiments is shown. (D) BM was treated as described in C, and Axl and Mertk mRNA levels were analyzed by quantitative RT-PCR. Bars represent mean (±SD). One representative out of two independent experiments is shown. (E) Representative confocal images of BMDMs from WT and TAM KO mice differentiated ± TGF-β1 and exposed to fluorescently labeled apoptotic thymocytes (AC). Cells were counterstained with rhodamine-phalloidin (actin cytoskeleton) and Hoechst (nuclei). Arrowheads indicate examples of AC uptake. Data are representative of three independent experiments. Bar, 50 µm. (F) Quantification of phagocytosis. Graphs show the mean (±SEM) normalized phagocytic index (number of engulfed ACs per number of macrophages). Data are representative of three independent experiments. T, Tyro3; A, Axl; and M, Mer; the combination represents the triple KO mouse. *, P < 0.05; ***, P < 0.001.

to that of humans (Figs. 1 D and 8 A). Specifically, Axl is expressed by keratinocytes and LCs as also observed in human epidermis (Fig. 8 A). In addition we detected Mer and Tyro3 by Western blot in total mouse epidermal lysates (Fig. 8 B). 1–2-mo-old TAM-deficient mice showed substantial reductions in epidermal LC frequencies (Fig. 8 C). When we looked into the complete TAM receptor KO system, we found these changes only in TAM triple-deficient mice but not in Axl single-deficient mice (Fig. 8 D), most likely because of the compensatory mechanisms described in Fig. 7 (A and B). Similar dose dependence of the phenotype has been previously observed in the TAM KO animals (Lu and Lemke, 2001). We also analyzed older TAM-deficient

mice (i.e., 5–12 mo). Interestingly these mice exhibited large patches of activated keratinocytes as indicated by high MHCII positivity (Fig. 8 E). LCs were abundantly present in areas of MHCII[hi] keratinocytes; conversely, areas lacking MHC[hi] keratinocytes showed diminished numbers of LCs. In fact we observed entire patches of skin from both aged and young TAM KO mice that were almost entirely depleted of LCs, with the sparse remaining cells being grossly enlarged (Fig. 8 C, right). In areas of inflamed skin of older TAM triple mutants, the dendritic epidermal T cells displayed a round appearance without dendrites, indicating an activated status, similarly as shown previously (Fig. 8 F, insets; Havran and Jameson, 2010).
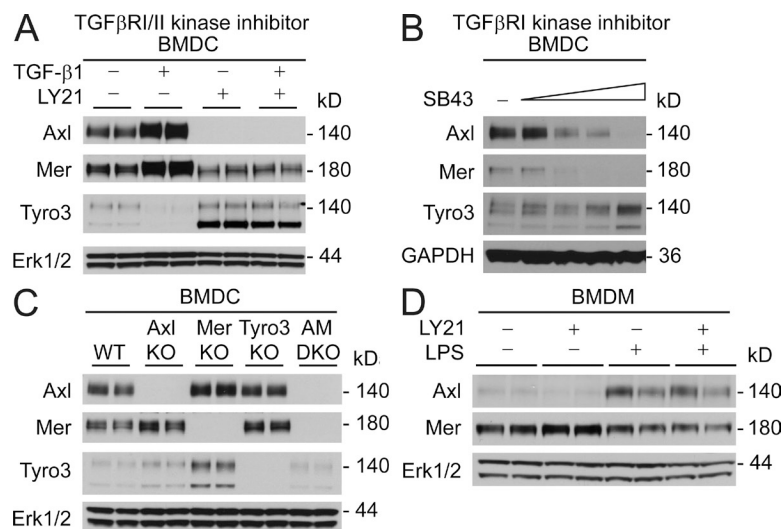
Figure 7. TGF–β1 signaling regulates TAM expression pattern by mouse BMDCs. (A) BM was cultured in the presence of GM-CSF ± TGF–β1 ± TGF–β receptor I/II kinase inhibitor (LY2109761) for 7 d and analyzed for TAM receptor expression by Western blot. (B) BM was cultured in the presence of GM-CSF and increasing concentrations of TGF–β receptor I kinase inhibitor (SB431542; 0.01, 0.1, 1, and 10 µM) for 7 d and analyzed for TAM receptor expression by Western blot. (C) BM from Axl, Mer, and Tyro3 single and Axl/Mer double KO mice was cultured in the presence of GM-CSF for 7 d and analyzed for TAM receptor expression by Western blot. (D) BMDMs were activated for 18 h with LPS in the presence or absence of LY2109761 and analyzed for Axl and Mer expression. (A, C, and D) Duplicate lanes represent separate differentiations. (A–D) Data are representative of two (B–D) or three (A) independent experiments.

Contact sensitizers activate Axl and up–regulate Mer in healthy human skin

Contact sensitizers such as $NiSO_4$ are known to induce cell death of epidermal cells and to activate DCs through human TLR4 when added in vitro and in vivo (Schmidt et al., 2010). To address whether the constitutively expressed Axl (Fig. 1 D) is phosphorylated in response to an activation signal, we treated isolated healthy human skin with $NiSO_4$ for 5 h and studied Axl activation. Anti–phospho–Axl, which detects the activated form of the receptor, fails to stain unstimulated skin (Fig. 9 A, top). In sharp contrast, tyrosine phosphorylation of Axl could readily be detected in $NiSO_4$–exposed LCs and to a lesser extent in keratinocytes (Fig. 9 A, bottom), whereas total Axl and Gas6 levels did not change appreciably (not depicted). Moreover, Tyro3 was not detectable in untreated or treated human epidermis (not depicted). However, hand in hand with Axl activation, LCs from $NiSO_4$–treated skin showed a marked up–regulation of Mer expression relative to low baseline levels in untreated skin (Fig. 9 B). In fact, Mer expression even allowed the specific identification of LCs in $NiSO_4$–exposed epidermis (Fig. 9 B, bottom). A comparable observation was made in human skin treated in parallel with the contact sensitizer 2,4 dinitro–1–fluorobenzene (DNFB) instead of $NiSO_4$ (not depicted).

Contact hypersensitivity (CHS) response augmented in mice lacking the TAM receptors

To study a potential role of the TAM receptors in the CHS response, TAM KO and WT mice were sensitized with DNFB on the shaved abdomen 5 d before ear challenge. Ear thickness was measured during the next 21 d as an indication of the inflammatory reaction. Ear swelling was more pronounced in TAM KO mice compared with WT. Moreover ear swelling continued to increase in TAM KO mice, unlike that observed for WT mice (Fig. 9 C). Fig. 9 D depicts representative ear sections 21 d after induction. Ears from TAM KO mice exhibited epidermal thickening and cellular infiltrates (Fig. 9 D).

DISCUSSION

In this study, we demonstrated that among human hematopoietic cells, Axl is strongly and specifically expressed by LCs and that Axl is the only TAM receptor detectable in these cells. Notably, human monocytes/macrophages lacked significant Axl and moDCs lacked detectable expression of all three TAM receptors. Furthermore, Axl is rapidly induced during LC commitment from $CD34^+$ hematopoietic progenitor cells, and FACS sorting of Axl^+ cells allowed the enrichment of LC-committed progenitors from these cultures. Axl expression is mediated by TGF–β1 signaling during LC commitment, and continuous TGF–β1 is required to maintain surface Axl expression by LC precursors, in keeping with a critical role of TGF–β1 during LC differentiation. Moreover, using mouse WT and specific TAM receptor–deficient mice, we demonstrated that TGF–β receptor I signaling induces Axl and represses Tyro3, therefore identifying a previously unrecognized counter-regulatory mechanism of Tyro3. Additionally, we provided evidence that this effect occurs independently of the here described compensatory regulation of the TAM system caused by the loss of individual receptors. We could show that Axl mediates antiinflammatory effects of TGF–β1 and identified the ability of TGF–β1 to increase AC clearance through the up-regulation of Axl. In human skin, we found the prominent expression, regulation, and activation of the TAM receptor system during steady-state and acute inflammation. Its importance in skin homeostasis is highlighted by the here observed impairment of the LC network and epidermal inflammation in mice lacking the TAM receptors. Together, these results represent important insights into the regulation and use of the TAM receptor system by TGF–β1 and implicate its dysregulation as a possible mechanism for autoimmune skin diseases.

Among leukocytes, expression of the TAM receptors is largely restricted to DCs and macrophages, where up-regulated Axl in particular has been proposed in negative feedback signaling downstream of TLR-induced type I IFNs during acute inflammation (Sharif et al., 2006; Rothlin et al., 2007).
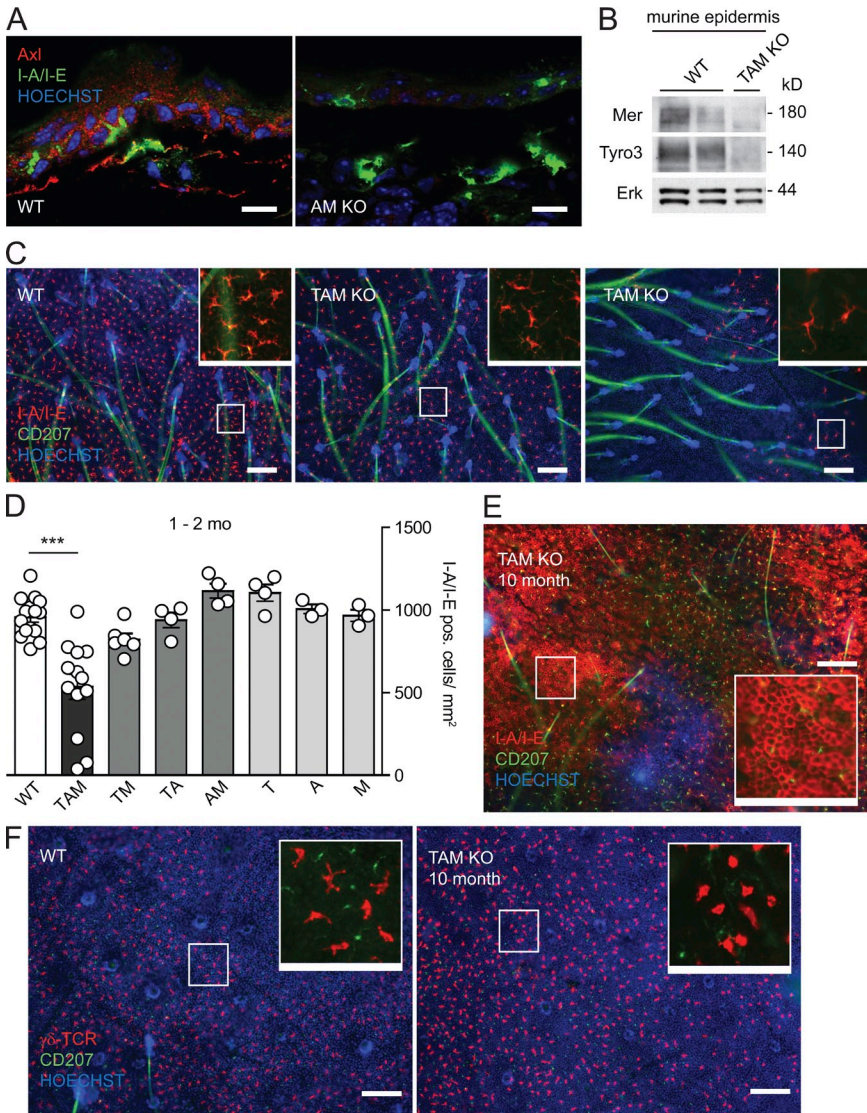
Figure 8. Loss of LC network integrity in TAM-deficient mice precedes skin inflammation. (A) Immunofluorescence staining of Axl in ear sections from WT and AM KO mice. Images are representative of three independent experiments. (B) Western blot analysis of epidermal protein lysates from two WT and one TAM KO mouse for Mer and Tyro3. Data are representative of two independent experiments. (C) Representative immunofluorescence staining of epidermal ear sheets from WT and two different TAM KO mice. LCs were visualized with Abs against I-A/I-E and CD207, and nuclei were stained with Hoechst. Colors are as indicated. Data are representative of more than three independent experiments. (D) I-A/I-E–positive cells from WT and TAM receptor KO mice were enumerated and shown in I-A/I-E+ cells/mm². Each dot represents one mouse. Bars indicate the mean ± SEM. ***, P < 0.001. (E) Representative image from an I-A/I-E–high region of a 10-mo-old TAM KO mouse. (F) Representative image of a 10-mo-old WT and TAM KO mouse. Dendritic epidermal T cells were visualized with Abs against the γδ-TCR. Colors are as indicated. T, Tyro3; A, Axl; and M, Mer; any combination represents the respective double or triple KO mouse. (C, E, and F) Insets represent higher magnifications of the framed areas. Bars: (A) 10 µm; (C, E, and F) 100 µm.

the growing evidence that Gas6 is the main ligand for Axl (Rothlin and Lemke, 2010; unpublished data).

During acute nickel–induced inflammation in healthy human skin explants, we observed rapid activation of Axl in LCs and keratinocytes (Fig. 9 A). Unexpectedly, Mer was up-regulated in this assay most dramatically in LCs, and to a lesser extent in keratinocytes (Fig. 9 B). A comparable observation was made when we used DNFB as contact sensitizer in human skin. In this regard it was remarkable to observe that DNFB caused an enhanced CHS response as well as a dramatically impaired resolution of this inflammatory reaction in TAM-deficient mice (Fig. 9 C). 3 wk after induction, most of the TAM KO mice still displayed severe skin swelling, strong dermal infiltration, and epidermal thickening (Fig. 9, C and D). This sheds light on a pathologically relevant human skin situation in vivo and highlights the mutual antiinflammatory action of the TAM receptors.

Lack of the TAM receptors in the steady state leads to phagocytic defects, impaired immune homeostasis, and spontaneous autoimmunity (Lu and Lemke, 2001). We here demonstrated that TGF-β1 induces Axl during cell differentiation and that TLR-induced Axl could not be inhibited by blocking TGF-β1 signaling, consistent with the hypothesis that these two pathways of Axl regulation are independent (Fig. 7 D).

We identified for the first time a prominent role for the TAM system in human skin. Axl, Mer, Gas6, and Protein S are constitutively expressed in the epidermis (Figs. 1 D and 2). Predominantly Axl and Gas6 were evident, and their suprabasal expression pattern mirrors that of TGF-β1 (Schuster et al., 2009). The gradual Axl expression along the epidermal TGF-β1 gradient indicates that the same regulatory mechanism is active during keratinocyte differentiation as here described for TGF-β1–instructed LC differentiation. The colocalization of Axl and Gas6 furthermore supports

Lack of the TAM receptors in mice can in rare occasions lead to spontaneous skin lesions similar to those observed in human autoimmune diseases (e.g., systemic lupus erythematosus; Lu and Lemke, 2001). We observed a lack of LC network integrity, as indicated by reduced LC numbers and the complete lack of LCs in some epidermal areas in TAM KO mice (Fig. 8, C and D). This phenomenon preceded the development of spontaneous skin inflammation, as observed from the
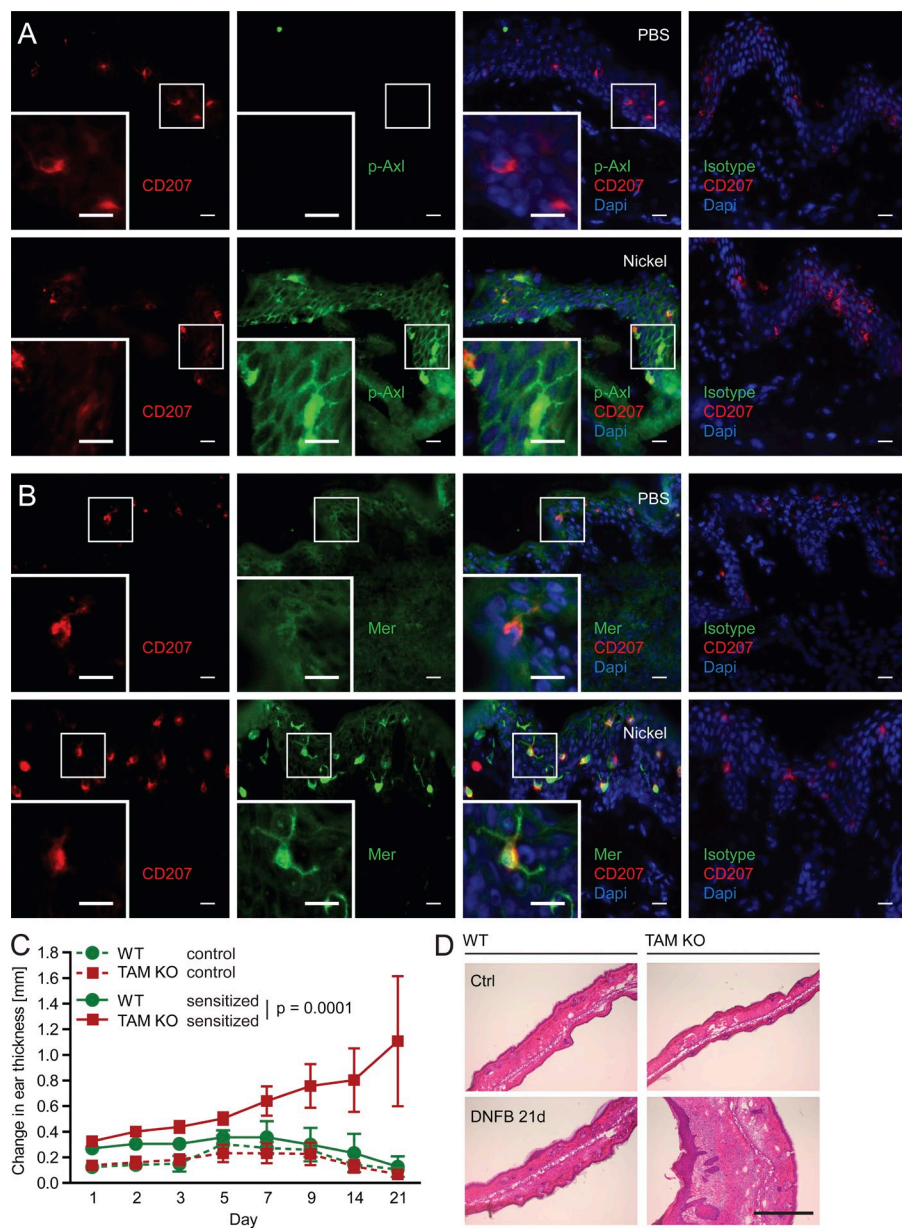
Figure 9. Effects of contact sensitizers on TAM receptors and their role during skin inflammation. (A and B) Human adult skin was cultured for 5 h at 37°C after the topical application of PBS or $NiSO_4$. Representative immunofluorescence stainings of cryosections for phospho-Axl (p-Axl; A) and Mer (B) are shown. LCs were visualized with Abs against CD207, and nuclei with DAPI. Pictures are representative of three different experiments performed with different donors. Colors are as indicated. The insets show an enlarged view of the framed areas. Section thickness was 5 µm. (C) TAM KO and WT mice were sensitized on the shaved abdomen with 0.5% DNFB. 5 d later, mice were challenged on one ear with 0.3% DNFB. Nonsensitized mice were challenged on one ear with 0.3% DNFB as control. The diagram shows the change in ear thickness at the indicated time points. Data are shown as mean ± SEM per time point (n = 5 mice per group). Data are pooled from two independent experiments. Statistical analysis for the whole dataset was performed using the two-way analysis of variance test. P-value is indicated. (D) Challenged mice from C were sacrificed 21 d after treatment, and ear sections were stained with hematoxylin and eosin. Data are representative of three mice per group. Section thickness was 11 µm. Bars: (A and B) 10 µm; (D) 1 mm.

large patches of MHC class II–positive keratinocytes and activated dendritic epidermal T cells in older triple mutants (Fig. 8, E and F). These observations argue against the possibility that the observed LC loss occurs secondary to skin inflammation. However, we cannot formally rule out this possibility. Although some Axl single KO mice showed a similar phenotype, it was most dramatic when the whole TAM system was abrogated, in line with previous observations made in these mice including auto-Ab production and several other manifestations of autoimmunity (Lu and Lemke, 2001).

The mechanism of constitutive Mer expression remains elusive. Macrophages seem to be able to up-regulate and switch to a Mer-dependent phagocytosis upon corticosteroid exposure (McColl et al., 2009). Here we showed that moLCs

and moDCs lack detectable Mer and that mouse BMDCs express this receptor at low levels. Mer seems to be the main phagocytosis receptor used by macrophages and indeed we could show its induction during macrophage differentiation in mice and man, confirming and extending previous observations (Seitz et al., 2007). An especially high and specific expression was observed during M2-driven macrophage differentiation from human monocytes under the control of M-CSF (Fig. 1 B; Verreck et al., 2004). We observed weak expression of Mer by $CD34^+$ cells and $CD34^+$ cell–derived LCs (Fig. 3 C). Human LCs in situ also expressed very low Mer levels (Fig. 9 B). The observation that Mer is strongly induced in LCs in response to $NiSO_4$ treatment indicates that Mer expression is a marker for activated LCs (Fig. 9 B).

Using BMDCs, we observed a strong counter-regulation of Tyro3 when we blocked endogenous TGF-β1–dependent Axl up-regulation. This observation is especially interesting because Tyro3 was otherwise expressed at very low levels in mouse DCs and macrophages and undetectable in human DCs, macrophages, or epidermis (Figs. 1 B, 3, 7, and not depicted). Even while part of this Tyro3 induction might be

attributed to the loss of Axl, as indicated by the phenotype of Axl single KO BMDCs, our data indicate that Tyro3 is actively repressed by TGF-βRI signaling (Fig. 7 B). Therefore, TGF-β1 is a general regulator of the TAM receptors. The analysis of TAM single mutants additionally highlights that the TAM system exhibits an interlinked self-regulation (Fig. 7 C), which underlines its importance in homeostasis and self-tolerance. In this context, it is interesting that we detected Tyro3 in mouse epidermal lysates, whereas it was undetectable in human epidermis (Fig. 8 B and not depicted). Therefore, slight differences in epidermal TAM receptor expression levels might exist between human and mouse.

We have identified a TGF-β1–mediated pathway regulating Axl expression during DC/macrophage differentiation. This pathway is independent of previously described TLR-induced Axl during inflammation (Fig. 7 D; Sharif et al., 2006; Rothlin et al., 2007). Apart from TGF-β1–rich tissues, such as the skin, TGF-β1 is produced from macrophages after PtdSer-dependent AC encounter, which occurs to a great extent after strong neutrophil influx for example in pneumonia or peritonitis (Huynh et al., 2002). TGF-β1 is the main antiinflammatory cytokine responsible for down-modulating these immune reactions and for mediating silent phagocytosis (Huynh et al., 2002). According to our data, enhancement of AC uptake and block of proinflammatory cytokines by DCs and macrophages that are exposed to TGF-β1 at the site of their differentiation (Figs. 5 and 6) may represent an Axl-dependent mechanism that ensures ongoing silent phagocytosis and prevents the development of autoimmune reactions. Indeed, the involvement of the TAM receptor system in human systemic lupus erythematosus has recently been demonstrated by increased soluble Axl and Mer and decreased Protein S serum levels, which are consistent with reduced TAM signaling in patients that display active disease (Suh et al., 2010; Ekman et al., 2011; Wu et al., 2011).

Apart from their implications in human autoimmune diseases, our findings may be of importance for cancer metastasis, where Axl appears to play an especially important role and where TGF-β1 signaling controls epithelial to mesenchymal transition (Zavadil and Böttinger, 2005; Linger et al., 2008). In this respect, the counter-regulation of Tyro3 that we report should be taken into account because TGF-β1 inhibitors are used in a variety of clinical trials (Flavell et al., 2010). Collectively, our results identify TGF-β1 as a master regulator of steady-state Axl expression. Additionally, we provide important new insights into the differential expression and self-regulation of the TAM system and its importance to the maintenance of cellular homeostasis and the resolution of inflammation in the skin.

MATERIALS AND METHODS

Isolation of primary human cells. Cord blood samples from healthy donors were collected during healthy full-term deliveries. CD34+ cells were isolated as described previously (Taschner et al., 2007). CD14+ monocytes were isolated from peripheral blood of healthy donors as described previously (Taschner et al., 2007). Human skin samples were obtained from healthy donors undergoing corrective surgery (breast reduction). Human epidermal single cell suspensions were prepared as described previously (Eisenwort et al., 2011). All procedures were performed in accordance with the guidelines from the Medical University of Vienna Institutional Review Board for these experiments. Informed consent was provided in accordance with the Declaration of Helsinki Principles.

Cytokines and reagents. Human stem cell factor (SCF), thrombopoietin (TPO), TNF, GM-CSF, fms-related tyrosine kinase 3 ligand (FLT3L), IL-6, IL-4, and human/mouse M-CSF were obtained from PeproTech; TGF-β1, IFN-γ, IL-1β, and recombinant human Gas6 were purchased from R&D Systems; mouse GM-CSF was from Akron Biotech, TGF-β receptor I/II inhibitor LY2109761 was provided by Eli Lilly and Company, and TGF-β receptor I inhibitor SB431542 was from GlaxoSmithKline. Ultrapure LPS from *Escherichia coli* and Pam₃CSK₄ was purchased from InvivoGen. The recombinant extracellular domain of Notch ligand Delta-1 fused to the Fc portion of human IgG1 (Delta-1ext-IgG) was provided by I. Bernstein (Fred Hutchinson Cancer Research Center, Seattle, WA). Coating of Delta-1ext-IgG was performed as previously described (Varnum-Finney et al., 2000; Heinz et al., 2006).

In vitro culture of primary human cells. CD34+ cord blood cells were cultured serum free for 2–3 d under progenitor expansion conditions (Flt3L, SCF, and TPO, each at 50 ng/ml) before subculturing with lineage-specific cytokines. LC cultures were described previously (Strobl et al., 1997). In brief, CD34+ cells (5 × 10⁴ to 10⁵/ml per well) were cultured in 24-well tissue culture plates in serum-free CellGro DC medium (CellGenix) supplemented with 100 ng/ml GM-CSF, 20 ng/ml SCF, 50 ng/ml Flt3, 2.5 ng/ml TNF, and 1 ng/ml TGF-β1 for 7 d. Cultures were supplemented with 2.5 mM GlutaMAX (Gibco/Invitrogen) and 125 U/ml each penicillin/streptomycin. CD14+ moDC and moLC cultures were described previously (Geissmann et al., 1998; Hoshino et al., 2005). In brief 10⁶/ml monocytes were seeded in 24-well tissue culture plates in RPMI 1640 medium (Sigma-Aldrich) supplemented with 10% FCS, 100 ng/ml GM-CSF, and 25 ng/ml IL-4 for moDC generation. MoLCs were generated either by adding 10 ng/ml TGF-β1 during MoDC cultures or in the presence of 100 ng/ml GM-CSF, Delta1 (coated plates as described above), and 10 ng/ml TGF-β1. Macrophages were generated either with 100 ng/ml GM-CSF or 100 ng/ml M-CSF for 5 d.

Mice and BM cultures. The generation of Axl, Mer, and Tyro3 single-, double-, and triple-KO mice has previously been described (Lu et al., 1999). All mice are of C57BL/6J × 129/Sv background. BM cells were isolated from tibias and femurs of 6–8-wk-old mice as described previously (Harding et al., 2010). Cells were differentiated for 7 d in RPMI containing 5% FBS (SAFC Biosciences) and antibiotic-antimycotic cocktail (Invitrogen). Differentiation media was supplemented with 100 ng/ml mM-CSF (for BMDMs), 20 ng/ml mGM-CSF (for BMDCs), or 20 ng/ml mGM-CSF + 20 ng/ml mM-CSF (for BM-derived LCs). Where indicated, 5 ng/ml TGF-β1 and/or 20 µM LY2109761 (Lacher et al., 2006) or various concentrations of SB 431542 were added to the cultures. The Animal Use Protocol (no. 09-030 and 11-00051) linked to the project titled "TAM Receptors in Innate Immunity" has been reviewed and approved by the Institutional Animal Care and Use Committee.

RNA isolation and real-time RT-PCR. RNA was isolated using RNeasy Mini kit (QIAGEN). 1 µg RNA was reverse transcribed using Transcriptor First Strand cDNA kit (Roche) and oligo (dT) primers. Quantitative PCR was run on ABI 7900HT (for mouse samples; Functional Genomics Facility, Salk Institute for Biological Studies) or Roche LightCycler (human samples) using the SYBR Green PCR Master Mix (Applied Biosystems) and indicated primers at 125 nM concentration. Primers for human Axl were described previously (Sun et al., 2002).

Primers for mouse cDNAs had the following sequences: Axl_F, 5′-TGAGCCAACCGTGGAAAGAG-3′; Axl_R, 5′-AGGCCACCTTATG-CCGATCTA-3′; Mertk_F, 5′-GATTCTGGCCAGCACAACAGA-3′;

Mertk_R, 5′-GAGATATCCGGTAGCCCACCA-3′; Gas6_F, 5′-AAC-TGGCTGAACGGGGAAG-3′; Gas6_R, 5′-CTTCCCAGGTGGTTT-CCGT-3′; ProS_F, 5′-CGCCGTGCAAATACCTTGTT-3′; ProS_R, 5′-AATGAGCCAACACGGAATGC-3′;Cyclophylin A_F,5′-AGACGC-CACTGTCGCTTTTC-3′; and Cyclophylin A_R, 5′-CTCCAGTGCT-CAGAGCTCGA-3′. Results were analyzed using the delta delta Ct method and presented as fold difference in mRNA level relative to Cyclophylin A (mouse samples) or HPRT (human samples; Livak and Schmittgen, 2001).

Flow cytometry. Flow cytometry staining and analysis were performed as described previously (Taschner et al., 2007). mAbs of the following specificities were used: FITC-conjugated mAbs specific for CD14, HLADR, CD1a, and CD86 (BD); PE-conjugated mAbs specific for CD207 (Beckman Coulter), HLADR; PerCP-conjugated anti-HLADR Ab (BD); allophycocyanin-conjugated Abs against CD1a, CD14 (BD), and CD324 (BioLegend); Pacific blue–conjugated mAbs against CD1a (BioLegend); and biotinylated mAbs specific for CD80, CD86, and CD11b (BD). Second step reagent was strep-tavidin (SA)-PerCP (BD). Axl, Mer, and Tyro3 were detected using mouse mAbs (R&D Systems) followed with a PE-conjugated anti–mouse second step Ab (Dako). Flow cytometric analysis was performed using an LSRII instrument (BD) and FlowJo software (Tree Star). For FACS sorting, the FACSAria flow cytometer (BD) was used.

Western blot analysis. Cells were lysed in lysis buffer containing 50 mM Tris-HCl, pH 7.5, 1 mM EGTA, 1 mM EDTA, 1% (wt/vol) Triton X-100, 0.27 M sucrose, 0.1% 2-mercaptoethanol, protease inhibitor cocktail (Roche), and phosphatase inhibitor cocktail (Roche). Protein concentration was measured using Bradford reagent (Bio-Rad Laboratories), and equal amounts of protein (5 µg) in LDS sample buffer (Invitrogen) were subjected to electrophoresis on a polyacrylamide gel and transferred to polyvinylidene fluoride membranes (Millipore). Membranes were blocked in TBS-T (50 mM Tris-HCl, pH 7.5, 0.15 M NaCl, and 0.25% [vol/vol] Tween 20) containing 5% (wt/vol) BSA. The membranes were then immunoblotted overnight at 4°C with primary Abs diluted 1,000-fold in blocking buffer. The blots were washed six times with TBS-T and incubated for 1 h at room temperature with secondary HRP-conjugated Abs diluted 5,000-fold in 5% (wt/vol) skimmed milk in TBS-T. After repeating the washing steps, signal was detected with the enhanced chemiluminescence reagent, and immunoblots were developed using an automatic film processor. Abs were used as follows: Mer (goat polyclonal; R&D Systems), Axl (goat polyclonal; M-20; Santa Cruz Biotechnology, Inc.), Tyro3 (goat polyclonal; C-20; Santa Cruz Biotechnology, Inc.), Gas6 (goat polyclonal; R&D Systems), and GAPDH (mouse monoclonal; Millipore).

Phagocytosis assay. LCs were generated from CD34+ cells as described previously (Strobl et al., 1997). Jurkat T cells were labeled with PKH26 dye according to the commercial protocol (Sigma-Aldrich) and seeded overnight in serum-free RPMI medium. To induce apoptosis, cells were UV irradiated with 800 mJ/cm² using a UV Stratalinker 1800 (Agilent Technologies) and further incubated at 37°C for 3 h. Apoptosis was analyzed by FACS using FITC-AnnexinV+/7AAD− staining. LCs were purified using 1 g sedimentation as described previously (Gatti et al., 2000). After cluster disruption with PBS/1 mM EDTA, LCs were incubated with 5 µg/ml blocking Axl Ab (R&D Systems) or goat isotype control for 30 min followed by incubation with the ACs at a density of 1:10. After 90 min, cells were washed three times with PBS/1 mM EDTA to remove nonengulfed cells. Cells were counterstained with CD1a to identify LCs and analyzed via FACS. CD1a-gated cells were evaluated for PKH26, and the percentage of CD1a/PKH26 double-positive cells was depicted. The macrophage phagocytosis assay was based on a previously described method (Scott et al., 2001). BMDMs were differentiated as described in Mice and BM cultures ± 0.25 ng/ml TGF-β1 and plated on glass coverslips the day before the assay. Thymocytes were isolated from syngenic mice and incubated with 2 µM Dex for 6 h to induce apoptosis. This results in 60–80%

ACs (FITC-AnnexinV+/7AAD−) and <1% necrotic cells (AnnexinV+/7AAD+). The cells were then washed and stained with green 5-chloromethylfluorescein diacetate (CMFDA) cell tracker. ACs were added to macrophages in 10-fold excess. After 1 h, cells were washed three times with PBS/0.1 mM EDTA to remove all nonengulfed cells and fixed with 4% paraformaldehyde. Cells were counterstained with rhodamine-phalloidin (actin cytoskeleton) and Hoechst (nuclei) and imaged at the confocal plane of cortical actin filaments to confirm internalization. For quantification in Fig. 6 F, single plane images were taken using a microscope (LSM 710; Carl Zeiss) with a Plan-Apochromat 20×/0.8 M27 objective. The quantification was performed using ImageJ software (National Institutes of Health). Representative images in Fig. 6 E are maximum intensity projections of z-stack images taken using an LSM 710 microscope with a Plan-Apochromat 63×/1.40 oil DIC M27 objective. Images were taken at the Waitt Advanced Biophotonics Center Core Facility, Salk Institute for Biological Studies.

Immunohistochemistry. Frozen human skin sections were stained as described previously (Göbel et al., 2009). For the detection of Axl and Gas6, affinity-purified goat Abs (1:100; R&D Systems) were used followed by a polyclonal donkey anti–goat Alexa Fluor 488–conjugated Ab (Invitrogen). Mer was detected using a rabbit mAb (1:100; Abcam) followed by a polyclonal goat anti–rabbit Alexa Fluor 488–conjugated Ab (Invitrogen). LCs were visualized with PE-conjugated mAbs specific for CD207 (Beckman Coulter). Nuclei were stained with DAPI, and slides were mounted using mounting medium (Dako). Pictures were taken using a microscope (Eclipse 80i; Nikon) and Lucia G software (Laboratory Imaging). Mouse epidermal ear sheets were prepared as described previously (Nagao et al., 2009). Epidermis was fixed in acetone, blocked with PBS containing 10% goat serum and 4% BSA, and stained with Abs against I-A/I-E (PE conjugated, 1:400; BioLegend) and CD207 (Alexa Fluor 488 conjugated, 1:300; Dendritics) to visualize LCs and Abs against γδ–TCR (PE-conjugated, 1:400; BD) to visualize dendritic-epidermal T cells, respectively. Nuclei were stained with Hoechst. Images from 10 randomly chosen microscopic fields were acquired. LCs were enumerated, and mean values were calculated per ear sheet. Axl was visualized in cryosections of mouse ears using goat anti-mAxl (R&D Systems).

Human skin explant cultures. Fresh human skin was cut into 0.5-cm² pieces and floated dermal side down on PBS in a 96-well plate. Skin samples were either treated atopically with 500 µM NiSO₄ and PBS as a control, respectively. After a 5-h incubation at 37°C, skin samples were prepared, stained, and processed as described in the previous section. For the detection of phosphorylated Axl, an affinity-purified rabbit anti–phospho-Axl (Y779) Ab (1:100; R&D Systems) was used.

CHS assay. Five male TAM KO mice and five age- and sex-matched WT control mice were shaved, and their abdomens were exposed to 0.5% DNFB (Sigma-Aldrich) in 4:1 acetone/olive oil (40 µl). After 5 d (sensitization phase), the baseline ear thickness was measured using a dial thickness gauge (Mitutoyo), and the left ear was treated on both sides epicutaneously with a 0.3% DNFB solution in acetone/olive oil (20 µl; elicitation phase). Ear thickness was measured at the indicated time points. The mice were euthanized after 3 wk. Morphological analysis was performed on 11-µm ear sections cut on a cryostat and stained with Mayer's hematoxylin and eosin Y.

Cytokine measurement. MoLCs were generated in the presence of 5 µg/ml blocking Axl Ab (R&D Systems) or goat isotype control. 0.5–1 × 10⁶/ml cells were activated with 1 µg/ml Pam₃CSK₄, and supernatants were collected 20 h later as described previously (Taschner et al., 2007). Cytokine (IL-6, IL-8, TNF, and IL-12p40) levels were quantified by using the Luminex system.

Statistical analysis. If not specified in figure legends, statistical analysis was performed using the paired or unpaired two-tailed Student's t test; p-values of <0.05 were considered significant.

JEM

REFERENCES

Anderson, H.A., C.A. Maylock, J.A. Williams, C.P. Paweletz, H. Shu, and E. Shacter. 2003. Serum-derived protein S binds to phosphatidylserine and stimulates the phagocytosis of apoptotic cells. *Nat. Immunol.* 4:87–91. http://dx.doi.org/10.1038/ni871

Borkowski, T.A., J.J. Letterio, A.G. Farr, and M.C. Udey. 1996. A role for endogenous transforming growth factor β 1 in Langerhans cell biology: the skin of transforming growth factor β 1 null mice is devoid of epidermal Langerhans cells. *J. Exp. Med.* 184:2417–2422. http://dx.doi.org/10.1084/jem.184.6.2417

Dang, H., A.G. Geiser, J.J. Letterio, T. Nakabayashi, L. Kong, G. Fernandes, and N. Talal. 1995. SLE-like autoantibodies and Sjögren's syndrome-like lymphoproliferation in TGF-beta knockout mice. *J. Immunol.* 155:3205–3212.

Eisenwort, G., J. Jurkin, N. Yasmin, T. Bauer, B. Gesslbauer, and H. Strobl. 2011. Identification of TROP2 (TACSTD2), an EpCAM-like molecule, as a specific marker for TGF-β1-dependent human epidermal Langerhans cells. *J. Invest. Dermatol.* 131:2049–2057. http://dx.doi.org/10.1038/jid.2011.164

Ekman, C., A. Jönsen, G. Sturfelt, A.A. Bengtsson, and B. Dahlbäck. 2011. Plasma concentrations of Gas6 and sAxl correlate with disease activity in systemic lupus erythematosus. *Rheumatology (Oxford).* 50:1064–1069. http://dx.doi.org/10.1093/rheumatology/keq459

Flavell, R.A., S. Sanjabi, S.H. Wrzesinski, and P. Licona-Limón. 2010. The polarization of immune cells in the tumour environment by TGFbeta. *Nat. Rev. Immunol.* 10:554–567. http://dx.doi.org/10.1038/nri2808

Gatti, E., M.A. Velleca, B.C. Biedermann, W. Ma, J. Unternaehrer, M.W. Ebersold, R. Medzhitov, J.S. Pober, and I. Mellman. 2000. Large-scale culture and selective maturation of human Langerhans cells from granulocyte colony-stimulating factor-mobilized CD34+ progenitors. *J. Immunol.* 164:3600–3607.

Geissmann, F., C. Prost, J.P. Monnet, M. Dy, N. Brousse, and O. Hermine. 1998. Transforming growth factor β1, in the presence of granulocyte/macrophage colony-stimulating factor and interleukin 4, induces differentiation of human peripheral blood monocytes into dendritic Langerhans cells. *J. Exp. Med.* 187:961–966. http://dx.doi.org/10.1084/jem.187.6.961

Göbel, F., S. Taschner, J. Jurkin, S. Konradi, C. Vaculik, S. Richter, D. Kneidinger, C. Mühlbacher, C. Bieglmayer, A. Elbe-Bürger, and H. Strobl. 2009. Reciprocal role of GATA-1 and vitamin D receptor in human myeloid dendritic cell differentiation. *Blood.* 114:3813–3821. http://dx.doi.org/10.1182/blood-2009-03-210484

Harding, C.V., D. Canaday, and L. Ramachandra. 2010. Choosing and preparing antigen-presenting cells. *Curr. Protoc. Immunol.* Chapter 16:Unit 16.1. http://dx.doi.org/10.1002/0471142735.im1601s88

Havran, W.L., and J.M. Jameson. 2010. Epidermal T cells and wound healing. *J. Immunol.* 184:5423–5428. http://dx.doi.org/10.4049/jimmunol.0902733

Heinz, L.X., B. Platzer, P.M. Reisner, A. Jörgl, S. Taschner, F. Göbel, and H. Strobl. 2006. Differential involvement of PU.1 and Id2 downstream of TGF-beta1 during Langerhans-cell commitment. *Blood.* 107:1445–1453. http://dx.doi.org/10.1182/blood-2005-04-1721

Hoshino, N., N. Katayama, T. Shibasaki, K. Ohishi, J. Nishioka, M. Masuya, Y. Miyahara, M. Hayashida, D. Shimomura, T. Kato, et al. 2005. A novel role for Notch ligand Delta-1 as a regulator of human Langerhans cell development from blood monocytes. *J. Leukoc. Biol.* 78:921–929. http://dx.doi.org/10.1189/jlb.1204746

Huynh, M.L., V.A. Fadok, and P.M. Henson. 2002. Phosphatidylserine-dependent ingestion of apoptotic cells promotes TGF-beta1 secretion and the resolution of inflammation. *J. Clin. Invest.* 109:41–50.

Kaplan, D.H., M.O. Li, M.C. Jenison, W.D. Shlomchik, R.A. Flavell, and M.J. Shlomchik. 2007. Autocrine/paracrine TGFbeta1 is required for the development of epidermal Langerhans cells. *J. Exp. Med.* 204:2545–2552. http://dx.doi.org/10.1084/jem.20071401

Kel, J.M., M.J. Girard-Madoux, B. Reizis, and B.E. Clausen. 2010. TGF-beta is required to maintain the pool of immature Langerhans cells in the epidermis. *J. Immunol.* 185:3248–3255. http://dx.doi.org/10.4049/jimmunol.1000981

Lacher, M.D., M.I. Tiirikainen, E.F. Saunier, C. Christian, M. Anders, M. Oft, A. Balmain, R.J. Akhurst, and W.M. Korn. 2006. Transforming growth factor-beta receptor inhibition enhances adenoviral infectability of carcinoma cells via up-regulation of Coxsackie and Adenovirus Receptor in conjunction with reversal of epithelial-mesenchymal transition. *Cancer Res.* 66:1648–1657. http://dx.doi.org/10.1158/0008-5472.CAN-05-2328

Lemke, G., and T. Burstyn-Cohen. 2010. TAM receptors and the clearance of apoptotic cells. *Ann. N. Y. Acad. Sci.* 1209:23–29. http://dx.doi.org/10.1111/j.1749-6632.2010.05744.x

Li, M.O., Y.Y. Wan, S. Sanjabi, A.K. Robertson, and R.A. Flavell. 2006. Transforming growth factor-beta regulation of immune responses. *Annu. Rev. Immunol.* 24:99–146. http://dx.doi.org/10.1146/annurev.immunol.24.021605.090737

Linger, R.M., A.K. Keating, H.S. Earp, and D.K. Graham. 2008. TAM receptor tyrosine kinases: biologic functions, signaling, and potential therapeutic targeting in human cancer. *Adv. Cancer Res.* 100:35–83. http://dx.doi.org/10.1016/S0065-230X(08)00002-X

Livak, K.J., and T.D. Schmittgen. 2001. Analysis of relative gene expression data using real-time quantitative PCR and the 2(-Delta Delta C(T)) Method. *Methods.* 25:402–408. http://dx.doi.org/10.1006/meth.2001.1262

Lu, Q., and G. Lemke. 2001. Homeostatic regulation of the immune system by receptor tyrosine kinases of the Tyro 3 family. *Science.* 293:306–311. http://dx.doi.org/10.1126/science.1061663

Lu, Q., M. Gore, Q. Zhang, T. Camenisch, S. Boast, F. Casagranda, C. Lai, M.K. Skinner, R. Klein, G.K. Matsushima, et al. 1999. Tyro-3 family receptors are essential regulators of mammalian spermatogenesis. *Nature.* 398:723–728. http://dx.doi.org/10.1038/19554

McColl, A., S. Bournazos, S. Franz, M. Perretti, B.P. Morgan, C. Haslett, and I. Dransfield. 2009. Glucocorticoids induce protein S-dependent phagocytosis of apoptotic neutrophils by human macrophages. *J. Immunol.* 183:2167–2175. http://dx.doi.org/10.4049/jimmunol.0803503

Nagao, K., F. Ginhoux, W.W. Leitner, S. Motegi, C.L. Bennett, B.E. Clausen, M. Merad, and M.C. Udey. 2009. Murine epidermal Langerhans cells and langerin-expressing dermal dendritic cells are unrelated and exhibit distinct functions. *Proc. Natl. Acad. Sci. USA.* 106:3312–3317. http://dx.doi.org/10.1073/pnas.0807126106

Nagata, K., K. Ohashi, T. Nakano, H. Arita, C. Zong, H. Hanafusa, and K. Mizuno. 1996. Identification of the product of growth arrest-specific gene 6 as a common ligand for Axl, Sky, and Mer receptor tyrosine kinases. *J. Biol. Chem.* 271:30022–30027. http://dx.doi.org/10.1074/jbc.271.47.30022

Ratzinger, G., J. Baggers, M.A. de Cos, J. Yuan, T. Dao, J.L. Reagan, C. Münz, G. Heller, and J.W. Young. 2004. Mature human Langerhans cells derived from CD34+ hematopoietic progenitors stimulate greater cytolytic T lymphocyte activity in the absence of bioactive IL-12p70, by either single peptide presentation or cross-priming, than do dermal-interstitial or monocyte-derived dendritic cells. *J. Immunol.* 173:2780–2791.

Riedl, E., J. Stöckl, O. Majdic, C. Scheinecker, K. Rappersberger, W. Knapp, and H. Strobl. 2000. Functional involvement of E-cadherin in TGF-beta 1–induced cell cluster formation of in vitro developing human Langerhans-type dendritic cells. *J. Immunol.* 165:1381–1386.

Rothlin, C.V., and G. Lemke. 2010. TAM receptor signaling and autoimmune disease. *Curr. Opin. Immunol.* 22:740–746. http://dx.doi.org/10.1016/j.coi.2010.10.001

Rothlin, C.V., S. Ghosh, E.I. Zuniga, M.B. Oldstone, and G. Lemke. 2007. TAM receptors are pleiotropic inhibitors of the innate immune response. *Cell.* 131:1124–1136. http://dx.doi.org/10.1016/j.cell.2007.10.034

Schmidt, M., B. Raghavan, V. Müller, T. Vogl, G. Fejer, S. Tchaptchet, S. Keck, C. Kalis, P.J. Nielsen, C. Galanos, et al. 2010. Crucial role for human Toll-like receptor 4 in the development of contact allergy to nickel. *Nat. Immunol.* 11:814–819. http://dx.doi.org/10.1038/ni.1919

Schuster, C., C. Vaculik, C. Fiala, S. Meindl, O. Brandt, M. Imhof, G. Stingl, W. Eppel, and A. Elbe-Bürger. 2009. HLA-DR+ leukocytes acquire CD1 antigens in embryonic and fetal human skin and contain functional antigen-presenting cells. *J. Exp. Med.* 206:169–181. http://dx.doi.org/10.1084/jem.20081747

Scott, R.S., E.J. McMahon, S.M. Pop, E.A. Reap, R. Caricchio, P.L. Cohen, H.S. Earp, and G.K. Matsushima. 2001. Phagocytosis and clearance of apoptotic cells is mediated by MER. *Nature.* 411:207–211. http://dx.doi.org/10.1038/35075603

Seitz, H.M., T.D. Camenisch, G. Lemke, H.S. Earp, and G.K. Matsushima. 2007. Macrophages and dendritic cells use different Axl/Mertk/Tyro3 receptors in clearance of apoptotic cells. *J. Immunol.* 178:5635–5642.

Sharif, M.N., D. Sosic, C.V. Rothlin, E. Kelly, G. Lemke, E.N. Olson, and L.B. Ivashkiv. 2006. Twist mediates suppression of inflammation by type I IFNs and Axl. *J. Exp. Med.* 203:1891–1901. http://dx.doi.org/10.1084/jem.20051725

Shull, M.M., I. Ormsby, A.B. Kier, S. Pawlowski, R.J. Diebold, M. Yin, R. Allen, C. Sidman, G. Proetzel, D. Calvin, et al. 1992. Targeted disruption of the mouse transforming growth factor-beta 1 gene results in multifocal inflammatory disease. *Nature.* 359:693–699. http://dx.doi.org/10.1038/359693a0

Stitt, T.N., G. Conn, M. Gore, C. Lai, J. Bruno, C. Radziejewski, K. Mattsson, J. Fisher, D.R. Gies, P.F. Jones, et al. 1995. The anticoagulation factor protein S and its relative, Gas6, are ligands for the Tyro 3/Axl family of receptor tyrosine kinases. *Cell.* 80:661–670. http://dx.doi.org/10.1016/0092-8674(95)90520-0

Strobl, H., E. Riedl, C. Scheinecker, C. Bello-Fernandez, W.F. Pickl, K. Rappersberger, O. Majdic, and W. Knapp. 1996. TGF-beta 1 promotes in vitro development of dendritic cells from CD34+ hemopoietic progenitors. *J. Immunol.* 157:1499–1507.

Strobl, H., C. Bello-Fernandez, E. Riedl, W.F. Pickl, O. Majdic, S.D. Lyman, and W. Knapp. 1997. flt3 ligand in cooperation with transforming growth factor-beta1 potentiates in vitro development of Langerhans-type dendritic cells and allows single-cell dendritic cell cluster formation under serum-free conditions. *Blood.* 90:1425–1434.

Suh, C.H., B. Hilliard, S. Li, J.T. Merrill, and P.L. Cohen. 2010. TAM receptor ligands in lupus: protein S but not Gas6 levels reflect disease activity in systemic lupus erythematosus. *Arthritis Res. Ther.* 12:R146. http://dx.doi.org/10.1186/ar3088

Sun, W.S., R. Misao, S. Iwagaki, J. Fujimoto, and T. Tamaya. 2002. Coexpression of growth arrest-specific gene 6 and receptor tyrosine kinases, Axl and Sky, in human uterine endometrium and ovarian endometriosis. *Mol. Hum. Reprod.* 8:552–558. http://dx.doi.org/10.1093/molehr/8.6.552

Tang, A., M. Amagai, L.G. Granger, J.R. Stanley, and M.C. Udey. 1993. Adhesion of epidermal Langerhans cells to keratinocytes mediated by E-cadherin. *Nature.* 361:82–85. http://dx.doi.org/10.1038/361082a0

Taschner, S., C. Koesters, B. Platzer, A. Jörgl, W. Ellmeier, T. Benesch, and H. Strobl. 2007. Down-regulation of RXRalpha expression is essential for neutrophil development from granulocyte/monocyte progenitors. *Blood.* 109:971–979. http://dx.doi.org/10.1182/blood-2006-04-020552

Ueno, H., E. Klechevsky, R. Morita, C. Aspord, T. Cao, T. Matsui, T. Di Pucchio, J. Connolly, J.W. Fay, V. Pascual, et al. 2007. Dendritic cell subsets in health and disease. *Immunol. Rev.* 219:118–142. http://dx.doi.org/10.1111/j.1600-065X.2007.00551.x

Varnum-Finney, B., L. Wu, M. Yu, C. Brashem-Stein, D. Staats, D. Flowers, J.D. Griffin, and I.D. Bernstein. 2000. Immobilization of Notch ligand, Delta-1, is required for induction of notch signaling. *J. Cell Sci.* 113:4313–4318.

Verreck, F.A., T. de Boer, D.M. Langenberg, M.A. Hoeve, M. Kramer, E. Vaisberg, R. Kastelein, A. Kolk, R. de Waal-Malefyt, and T.H. Ottenhoff. 2004. Human IL-23-producing type 1 macrophages promote but IL-10-producing type 2 macrophages subvert immunity to (myco)bacteria. *Proc. Natl. Acad. Sci. USA.* 101:4560–4565. http://dx.doi.org/10.1073/pnas.0400983101

Wu, J., C. Ekman, A. Jönsen, G. Sturfelt, A.A. Bengtsson, A. Gottsäter, B. Lindblad, E. Lindqvist, T. Saxne, and B. Dahlbäck. 2011. Increased plasma levels of the soluble Mer tyrosine kinase receptor in systemic lupus erythematosus relate to disease activity and nephritis. *Arthritis Res. Ther.* 13:R62. http://dx.doi.org/10.1186/ar3316

Zavadil, J., and E.P. Böttinger. 2005. TGF-beta and epithelial-to-mesenchymal transitions. *Oncogene.* 24:5764–5774. http://dx.doi.org/10.1038/sj.onc.1208927